Electrolyte Modulation Strategies for High Performance Zinc Batteries
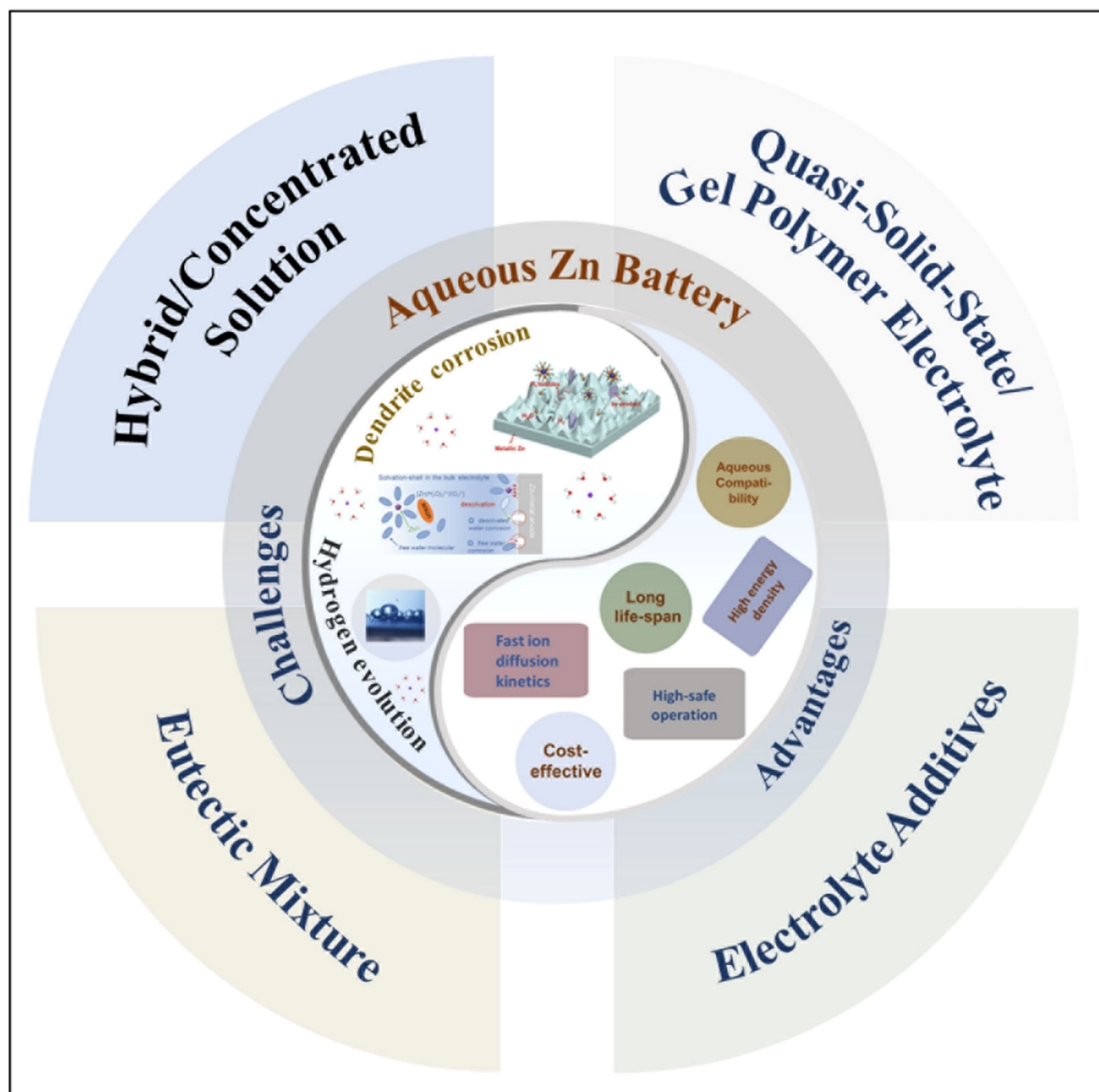
Mingming Han,[a] Tian Chen Li,[b] Dong-Sheng Li,[c] and Hui Ying Yang*[b]

Batteries & Supercaps

Review
doi.org/10.1002/batt.202200560

Chemistry Europe
European Chemical
Societies Publishing

With high safety and low-cost features, aqueous zinc batteries have become the promising rechargeable battery technology for future. Recent research works reached a deep understanding on the underlying electrolyte chemistry in Zn batteries. This review aims to put forward the challenges that the aqueous electrolyte is facing, which include low voltage window, multifarious irreversible reactions, and low energy density. The innovative electrolyte modulation strategies, such as hybrid/concentrated solution, gel polymer electrolyte (hydrogel electrolyte), eutectic mixture, electrolyte additives, towards better zinc batteries performance are summarized. The conclusion and outlook are introduced to provide guidance for smart design of electrolyte for advanced Zn batteries.

1. Introduction of Aqueous Zinc Battery

The rising environmental concerns and energy demands call for clean and effective energy storage and conversion devices for sustainable development.[1] Secondary metal-ion battery technology is an attractive electrochemical energy storage and conversion (EESC) device due to its high energy density, long life-span and environmental friendliness.[2] The extraordinary activity of alkali metals, flammability of organic electrolyte and the expense of scarce resources (e.g., Ni, Co and Li) of lithium-/sodium-/potassium-ion battery (LIB/SIB/KIB) present various safety hazards and economic challenges.[3] Alternative battery candidates using abundant components (metal anode and cathode material) with high energy density and high safety are appealing.[4] Among the abundant metals in the earth's crust, Mg, Ca, Al and Zn are non-toxic and possess high energy densities, which make them the desirable metal anodes. Multivalent metal-ion batteries (MIBs), especially the aqueous systems based on these metals change from the metal ion- to metal-anode-based system, accompanying with the multivalent charge carriers shuttling back and forth between electrodes.[5] Some special physic-chemical properties are summarized in Figure 1(a). Therefore, MIBs are a key battery technique for further exploration on future EESC applications.

Noteworthy, the successful operation of multivalent metals in battery system depends significantly on the electrolyte solution.[6] The atmospheric components, protic solvent, polar aprotic solvent and some anions could react easily with Mg, Ca and Al, which leads to severe passivation on metal surface.[7] Sluggish transfer kinetic and unclear mechanism of Mg^{2+}, and severe dendrites growth at metal anode side (Ca and Al) further limits their practical application.[8] Aqueous Zn-ion batteries (AZIBs) based on Zn metal are receiving much attentions as a safe and effective electrochemical technology due to the non-flammability, low-toxicity and high-conductivity of aqueous solution[9] (Figure 1b). Furthermore, the high capacities (819 mAh g^{-1}, 5851 mAh mL^{-1}), relatively low redox potential (−0.76 V vs. SHE) and the high Columbic efficiency (CE) during its plating/stripping of Zn anode drive the recent renaissance of rechargeable Zn batteries development.[10] Even though the impressive electrochemical performance has been achieved and the underlying energy storage mechanism has been characterized significantly,[11] AZIBs still suffer from relatively low energy density and insufficient cycling stability due to the narrow operating voltage range and severe side reactions of aqueous system.[12] This short review aims to present a summary on the issues of the aqueous electrolyte and the corresponding strategies on modulating electrolyte.

2. Issues of Electrolyte and Anode

Fundamentally, there is the thermodynamic stability of water which determines the oxygen evolution reaction (OER) and hydrogen evolution reaction (HER) potentials.[12c,13] The potential difference between OER and HER of water is electrochemical stability window (ESW). It is approximately 1.23 V (Figure 1c). Considering the sluggish reaction kinetics of OER and HER at the electrode interface, the practical ESW is usually higher than 1.23 V, but lower than 2 V.[14] In addition, even trace amounts of O_2/H_2 can deteriorate the electrode structure, consume electrolyte solution and cause severe self-discharging.[15] This issue restraints the operating output voltage of aqueous battery systems and causes insufficient cycling stability.[16]

The platting/stripping efficiency of Zn anode and platting morphology of Zn metal in aqueous solution are also important parameters for battery safety.[17] In general, the platting/stripping efficiency is determined by solvation/de-solvation energies, ion diffusion process, liquid/solid-phase mass and charge transfer kinetics. However, the high de-solvation energy barrier of the $[Zn(H_2O)_6]^{2+}$, the high activity of water molecules and Zn metal, and the concentration/electrical field polarizations make the platting/stripping procedure complicated with undesirable efficiency.[18] The side reactions are shown in Figure 1(d), which includes hydrogen evolution reaction, taking place before Zn deposits with irreversible by-products (e.g., $Zn(OH)_2$, ZnO) formed; Zn anode corrosion, occurring in humid atmosphere; dendrites formation, arising from the hostless

[a] Dr. M. Han
     Hangzhou Institute of Advanced Studies
     Zhejiang Normal University
     Jinhua (China)
[b] T. C. Li, Prof. H. Y. Yang
     Pillar of Engineering Product Development
     Singapore University of Technology and Design
     8 Somapah Road, Singapore 487372 (Singapore)
     E-mail: yanghuiying@sutd.edu.sg
[c] Dr. D.-S. Li
     College of Materials and Chemical Engineering
     Key Laboratory of Inorganic Nonmetallic Crystalline and Energy Conversion
     Materials
     China Three Gorges University
     Yichang, 443002 (China)

Batteries & Supercaps

Review
doi.org/10.1002/batt.202200560

Chemistry Europe
European Chemical
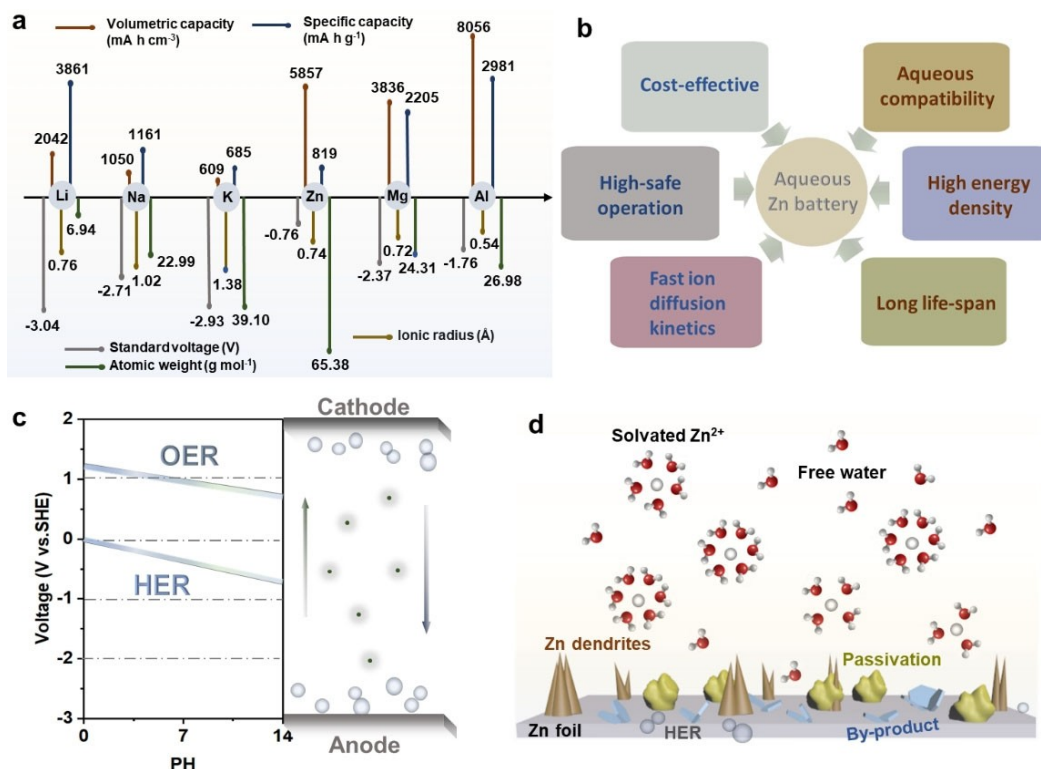Societies Publishing

Figure 1. a) Comparisons of different metal ions on the physic-chemical properties; b) Schematic illustration of the advantages of aqueous Zn battery; c) Pourbaix diagram of HER and OER in aqueous solutions; d) Zn^{2+}-solvated structures and Zn/electrolyte interface side reactions in dilute aqueous electrolyte.

nature of Zn metal.[19] The favorable morphology of Zn deposits for battery operation is homogeneous and densely-packed crystals with conformity. Even though the weak acid aqueous electrolyte could contribute to less detrimental interconnected platelets than that in alkaline solutions at some extent, the porous Zn deposits with irregular morphologies composed with hexagonal platelets are extensively demonstrated. The loose Zn particles could deteriorate the conductivity of anode and pierce the separator, leading to cycling instability and short circuits.[20]

Mingming Han completed her Ph.D. from Central South University in Material Science and Chemistry, where her focus was on the aqueous Zn-Mn battery and eutectic electrolyte design in Zn battery. Currently, she is working as a young lecturer in Hangzhou Institute of Advanced Studies, Zhejiang Normal University. Her research direction is aqueous Zn battery and eutectic electrolyte design.

Tian Chen Li received his master's degree (2019) in Materials Science and Engineering from Central South University. He is now a PhD student in the Pillar of Engineering Product Development, SUTD, under the supervision of Prof. Hui Ying Yang. His research mainly focuses on zinc-ion electrolytes and electrode/electrolyte interface.

Dong-Sheng Li is currently a professor in the College of Materials and Chemical Engineering at the China Three Gorges University. His research directions are clean energy production/storage/conversion materials, the treatment of greenhouse gases and the sensing detection and degradation of pollutants, and the purification of key chemicals in microelectronics.

Hui Ying Yang is currently a professor in the pillar of Engineering Product Development at the Singapore University of Technology and Design. Her current research interests are advanced materials science, such as function engineering and chemical doping in low dimensional nanomaterials, for a variety of high-efficient devices and technologies with applications in sustainable energy and environment.

3. Promising Ways Forward

3.1. Hybrid/concentrated solution

The excessive free water molecules and the strong Coulombic interactions between the Zn^{2+} ions and their surrounding solvated water accelerate the parasitic side reactions.[18b,21] Decreasing the water solvent content and weakening the bonding strength between Zn^{2+} ion and water molecules through replacing water solvent with organic counterpart would improve Zn plating/stripping efficiency, broaden the ESW and suppress cathode dissolution.[22] It is confirmed that a highly reversible Zn deposition behavior of Zn metal ($\geq$ 99.0%) and high anodic stability (~3.6 V vs. Zn) is achieved in organic electrolytes, e.g., (acetonitrile) AN–$Zn(TFSI)_2$,[23] AN–Zn-$(CF_3SO_3)_2$,[24] DMC-TMP–$Zn(TFSI)_2$ (dimethyl carbonate-trimethyl phosphate).[25] Recently, Xu et al.[26] have discovered a class of nonaqueous but protic solvent based on the alcohol family. Taking the MeOH as an example, Figure 2(a) demonstrates that the Zn^{2+} ion pairs is tuned by MeOH solvent and OTf$^-$ anion. Both the Molecular Dynamic (MD) calculations and experimen-

tal results confirm the satisfying dynamic property of the Zn^{2+} transference number in this organic electrolyte (Figure 2b). When the molar ratio between $Zn(OTf)_2$ and MeOH is 14:1, Zn metal electrode could plate/strip reversibly with $\geq$ 99.5% CE, and Zn//Zn symmetric cell could run for 1800 hours without short-circuit. The deep explorations (TEM and XPS spectra, Figure 2c–f) on interfacial chemistry of Zn electrode after cycling (20 and 200 hours) uncover that a nanometer scale interface layer with ZnS, $ZnSO_3$, and ZnF_2 components forms. It explains the mechanism behind the exceptional electrochemical performance and provide insight on low-cost and sustainable battery chemistry. Considering the sluggish diffusion kinetics of organic solvent, hybrid solution containing water and organic co-solvent would be an ideal choice.[27] One good example is the (triethyl phosphate) TEP-H_2O) co-solvent.[28] Combining with $Zn(CF_3SO_3)_2$ salt, the Zn//Zn symmetric cell could plate/strip for 3000 hours with a high CE of 99.68% in Zn//SS (stainless steel) asymmetric cell. However, the detailed discussion on the fundamental understandings (e.g., solvation structure, ion diffusion mechanism, chemical environment) about the hybrid solution has not been given. Another
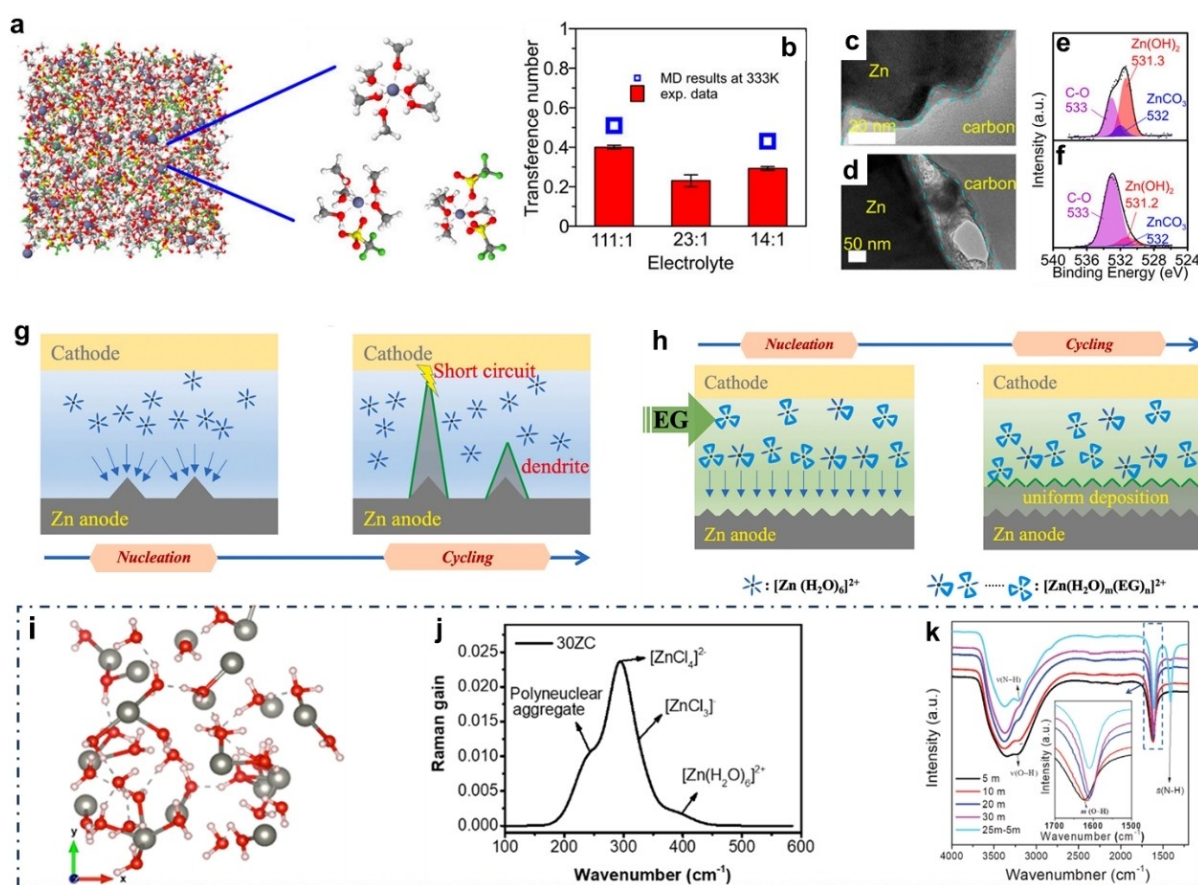

Figure 2. a) Snapshot of the MD calculation box with the Zn-clusters and b) Zn^{2+} transference number in the MeOH–$Zn(OTf)_2$ organic electrolyte; c, d) TEM images of Zn surface after cycling (20 and 200 hours, respectively); e, f) XPS spectra of Zn surface after cycling (20 and 200 hours, respectively). Adapted from Ref. [26]. Copyright (2022) the Author(s). Published by PNAS. Comparison of Zn deposition and growth process in g) Common $ZnSO_4$ electrolyte and h) $ZnSO_4$/ EG hybrid electrolyte. Adapted with permission from Ref. [29]. Copyright (2020) Elsevier. i) Ab initio molecular dynamic calculations and the corresponding snapshot of 30 m $ZnCl_2$; j) Femtosecond stimulated Raman spectra of 30 m $ZnCl_2$ electrolyte. Adapted from Ref. [12b]. Copyright (2020) The Author(s). Carbon Energy published by Wenzhou University and John Wiley & Sons Australia, Ltd. k) FTIR spectra of $ZnCl_2 + NH_4Cl$ mixed electrolytes with different concentrations. Adapted with permission from Ref. [31a]. Copyright (2020) Wiley-VCH.

Batteries & Supercaps

Review
doi.org/10.1002/batt.202200560

Chemistry
Europe
European Chemical
Societies Publishing

following work has characterized the structure of (ethylene glycol) EG-H$_2$O hybrid solution.[29] It points out that the strong hydrogen bonding between EG and H$_2$O, and the solvation interplay between Zn^{2+} and EG, could break the interactions among water molecules and change the solvation structure of Zn^{2+}. As Figure 2(g and h) shows, the [Zn(H$_2$O)$_6$]$^{2+}$ ion with fast diffusion tends to aggregate and form dendrite in EG-free electrolyte. While the [Zn(H$_2$O)$_m$(EG)$_n$]$^{2+}$ ion deposits into Zn nuclei with smaller size and diffuses with 3D pathway in EG-H$_2$O hybrid electrolyte, which is due to the decreased diffusion and increased nucleation over-potential. Thus, the suppressed hydrogen evolution reaction, homogeneously dense-packed Zn deposits and long-term cycling performance are obtained.

The "water-in-salt" concentrated electrolyte, where the free water number available to solvate with cations is far below than the "solvation number" in conventional electrolyte, is supposed to form anion-containing solvation sheath and expand the ESW of aqueous solution to ~3 V.[14] It is reported that the Mo$_6$S$_8$//LiMn$_2$O$_4$ full cell using 21 m LiTFSI electrolyte delivers an open circuit voltage of 2.3 V and cycles at ~100% coulombic efficiency up to 1000 cycles. Apart from the decreased free water amount, the Li$_2$(TFSI)(H$_2$O)$_x$ aggregates derived solid interface at electrode surface plays a vital role on the stable operation of the electrochemical processes. In 2018, it is also proved that the Zn metal anode could plate and strip with 100% CE and deposits with dendrite-free morphology in another concentrated electrolyte (1 m Zn(TFSI)$_2$ + 20 m LiTFSI).[30] Similarly, the high populations of anions force them enter into the Zn^{2+} vicinity forming cation-anion aggregates (Zn-(TFSI)$_m$-(H$_2$O)$_n$). With the concentration increasing, the Zn^{2+} solvation structure changes from the original [Zn(H$_2$O)$_6$]$^{2+}$ in dilute solution to [Zn(TFSI)$_n$] composition in concentrate solution. The significantly decreased Zn-(H$_2$O)$^+$ clusters and unique solvation structure enable unprecedented flexibility and reversibility to Zn batteries. Combining with LiMn$_2$O$_4$ and O$_2$ cathode, high energy densities of 180 and 300 Wh kg^{-1} are obtained, respectively. TFSI$^-$-based salt is thought as desirable choice for concentrated solution but at the expense of high cost. Then, concentrated ZnCl$_2$-based solutions[12b,31] (e.g., 30 m ZnCl$_2$, 30 m ZnCl$_2$+5 m LiCl, 25 m ZnCl$_2$+5 m NH$_4$Cl) are discovered in following works. Various characterizations further verified that the anion-containing solvation structures (e.g., [Zn(OH$_2$)$_2$Cl$_4$]$^{2-}$, [ZnCl$_4$]$^{2-}$) domain the Zn^{2+}-species, and the hydrogen bonding reactions among water molecules are significantly decreased (Figure 2i–k). They guarantee the stable plating/stripping behavior of Zn metal, compact dendrite-free Zn deposits and suppressed hydrogen evolution.

3.2. Gel polymer electrolyte (hydrogel electrolyte)

The constraints of aqueous electrolyte have fostered the development of another kind of gel polymer electrolyte (GPE). In this review, we mainly focus on the hydrogel electrolyte. It is usually prepared through incorporating metal salt solution into the polymer matrix which is synthesized through *in-situ/ex-situ* ways *via* ionic/covalent crosslinks.[32] Some representative syn-

thesis procedures and inner structures of GPE are shown in Figure 3(a–c). GPEs both have the special mechanical properties (flexibility, stretchability and foldability) of solid-state electrolyte and diffusion characters of aqueous electrolyte.[33] The low crystallinity of polymers and the high amorphous ratio of GPE enable the conductivity keeps a high value (10^{-3}–10^{-4} S cm^{-1}). The fundamentals that the strong hydrogen bonds formed between hydrophilic functional groups (e.g., hydroxyl, carbonyl, sulfonic and amino groups) on polymer matrix and water molecules, decreases the amount of free water and suppresses cathode dissolution significantly; and the molecular interactions between the functional groups and Zn^{2+} ion, makes sure the well-ordered ion diffusion and the corresponding homogeneously deposition of Zn.[34] There are different kinds of polymer composites as the host systems of GPEs owing to their high dielectric constant and compatibility, such as PEO, PVA, PAA, PAM, PVDF, cellulose, gelation.[33a,35] In general, GPEs could act as both the electrolyte and separator, being the prime choice for the flexible electrical devices.

During the past 10 years, many works have confirmed the effects of GPEs on solving parasitic issues in Zn batteries. For example, the reported PVA-ZnCl$_2$ hydrogel,[41] gelatin-PAM hierarchical polymer hydrogel,[42] PAAm/alginate-Zn hydrogel[37] and Zn(CF$_3$SO$_3$)$_2$-PVDF-HFP[34b] hydrogel electrolytes. They extend the electrochemical stable voltage (~3 V) greatly through decreasing the water solvent ratio and strengthening hydrogen bonding reaction between polymer and water molecules; contribute to the ordered diffusion of Zn^{2+} and the uniform deposition of Zn through the Zn^{2+}-confinement effect of polymer matrix; and finally improve the cycling stability (up to thousands of cycles) of the battery through suppressing side reactions on electrode and electrolyte sides[39,40] (as shown in Figure 3d, e). Various works where the polymer modification, biopolymers and functional additives addition are reported, which enriches the GPEs family significantly. The typical methods of modifying polymer hydrogel with unique mechanical properties (e.g., stretchability, compressibility and self-healing ability) are crosslinking agent-assistant synthesis, self-assembly, templated synthesis and interpenetrating polymeric network and so on.[34b] One good example of polyacrylamide-alginate dual-ion crosslinked hydrogel is reported by Suo and co-workers. The ionically (alginate ionic chain) and covalently (polyacrylamide chain) crosslinked networks in this hydrogel contribute to the high fracture energy (9000 J m^{-2}) and the self-healing ability synergy.[43] Last year, Zhou and co-workers[44] developed an integrated "all-in-one" electrode through the combination of 3D structural design (Cu foam@Zn), interface modification, and electrolyte optimization (the structure and function mechanism of this electrode is shown in Figure 4). The as-prepared electrode coated with hydrogel electrolyte (palygorskite-Sodium alginate-ZnSO$_4$) suppressed gas evolution and water-driven side reactions with a 600 hours long-time stability almost without polarization. Multifunctional polymers extracted from natural plants have caught considerable attentions because of the potential of biocompatible materials. As reported that the zwitterionic sulfobetaine-cellulose hydrogel electrolyte,[45] in which both the zwitterionic sulfobetaine and
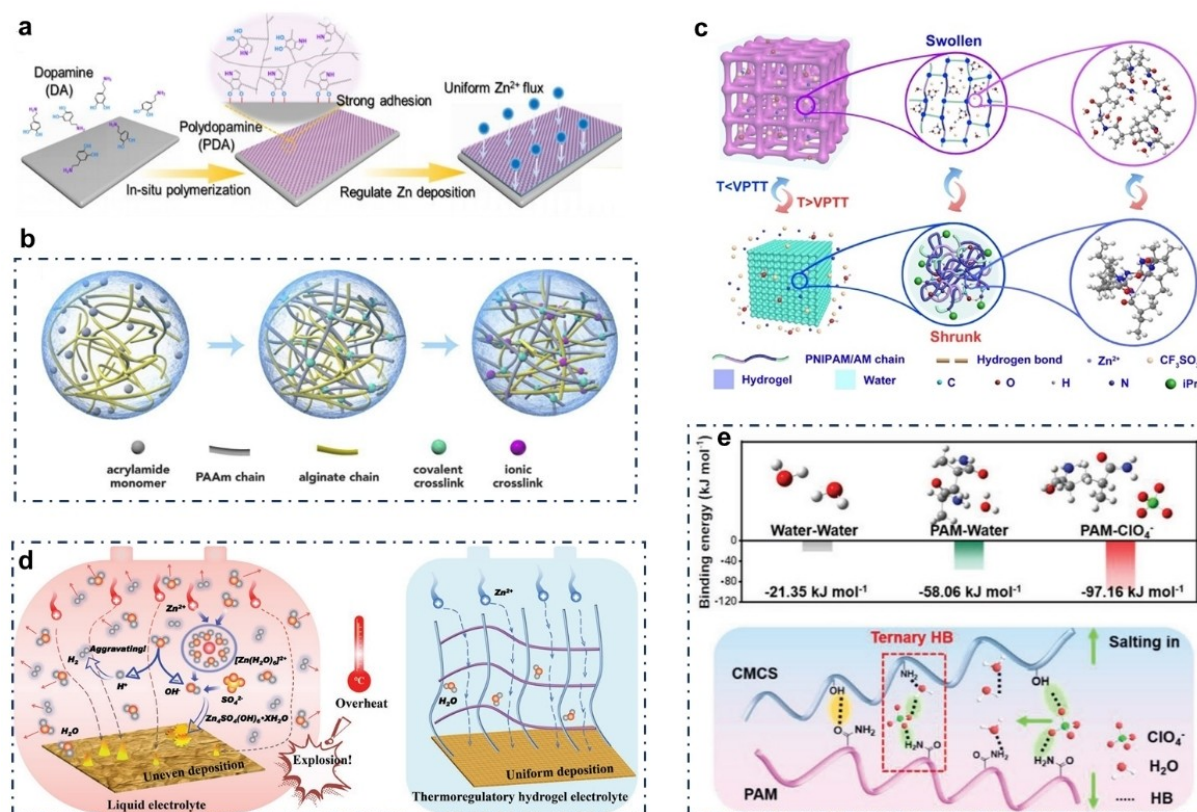
Figure 3. a) Scheme of the *in-situ* synthesis procedure of the polymer interface layer on Zn anode and its effective mechanism for Zn^{2+} flux diffusion. Adapted with permission from Ref. [36]. Copyright (2021) Royal Society of Chemistry. b) PAAm-alginate hydrogel structure evolution, in which covalent and ionic crosslinks exist. Adapted with permission from Ref. [37]. Copyright (2019) Elsevier B.V. c) Working mechanism of the thermal-gated PNIPAM/AM electrolytes with VPTT. Adapted with permission from Ref. [38]. Copyright (2020) Wiley-VCH. d) Schematic of the side reactions in common liquid and thermoregulatory hydrogel electrolyte. Adapted with permission from Ref. [39]. Copyright (2022) Wiley-VCH. e) DFT optimized structures in the CSAM–C hydrogel and the schematic diagram of the interactions among CMCS, ClO$_4^-$, and PAM chains in CSAM–C hydrogel. Adapted with permission from Ref. [40]. Copyright (2023) Wiley-VCH.

cellulose raw materials are obtained from the natural plants. Taking the advantages of the numerous charged zwitterionic chains, on which the anionic and cationic counterions could be separated during charging/discharging process, facilitates fast Zn^{2+} ion transport. Meanwhile, the charged and polarized zwitterionic groups enhances electrode/hydrogel interface adhesion ability and contributes to the formation of hydrogel matrix. Combining with cellulose nanofibrils, which acts as both the mechanically reinforcing additive and hydrophilic skeleton, the semi-interpenetrating hydrogel network is obtained. It is demonstrated that the solid-state Zn//MnO$_2$ battery using this electrolyte exhibits a very high-rate performance (275 mAh g^{-1} at 1 C, 74 mAh g^{-1} at 30 C) and an ultra-stable cycling performance (10,000 cycles).

It is well-accepted that the ionic conductivity plays a vital role in GPE, but it is still a challenge to achieve a desirable value. Functional additives, such as oxide nanoparticles, ionic liquid, active plasticizer (PC/EC solvent), could facilitate the migration of Zn^{2+} through interacting with polymer.[32] As reported by Johnsi,[46] who prepared a GPE composed of Zn(CF$_3$SO$_3$)$_2$ and PVDF-HFP, the conductivity reaches 3.4×10^{-4} S cm^{-1} with the largest Zn^{2+} transport number of 0.57 when the 5 wt% TiO$_2$ nanofiller is added. Replacing TiO$_2$ with

ZrO$_2$, the conductivity of 4.6×10^{-4} S cm^{-1} is obtained. Guisao and co-workers[47] fabricated another GPE composed of PVDF-HFP, EMIMTFSI, Zn(OTf)$_2$ and n-methyl-2-pyrrolidone (NMP), in which the Zn^{2+} could transfer along the polymer chains with a transfer number of 0.575. Based on this GPE, the Zn-MnO$_2$ battery delivers a discharge capacity of 125 mAh g^{-1}. In addition, the Zn//β-MnO$_2$ battery using Zn(OTf)$_2$-PEGDGE-PC antiaging solid-state electrolyte exhibits a discharge capacity of 177 mAh g^{-1} with the retention of 85% after 300 cycles at an ionic conductivity of 3.77×10^{-4} S cm^{-1}.[48] Additionally, Vijayakumar et al. further confirm the high conductivity of 10^{-3} S cm^{-1} of Zn(OTf)$_2$-PC-2-hydroxy-2-methylpropiophenone in Zn//VOPO$_4$ battery. Noteworthy, a wide electrochemical stable voltage of 2.4 V with the high average operating voltage of 1.2 V and 87% capacity retention after 600 cycles are obtained.[49] Besides the quasi-solid-state/gel polymer electrolyte, other polymer based all-solid-state (e.g., PEO–Zn-(CF$_3$SO$_3$)$_2$)-ZnO,[50] PEO-PVdF–Zn(CF$_3$SO$_3$)$_2$[51]) and inorganic colloidal gel[52] (e.g., palygorskite added in ZnSO$_4$ solution, bentonite added in ZnSO$_4$ solution) electrolytes are also reported, which boost the development of high-performance Zn battery greatly and give guidelines on designing functional polymer gel electrolyte.
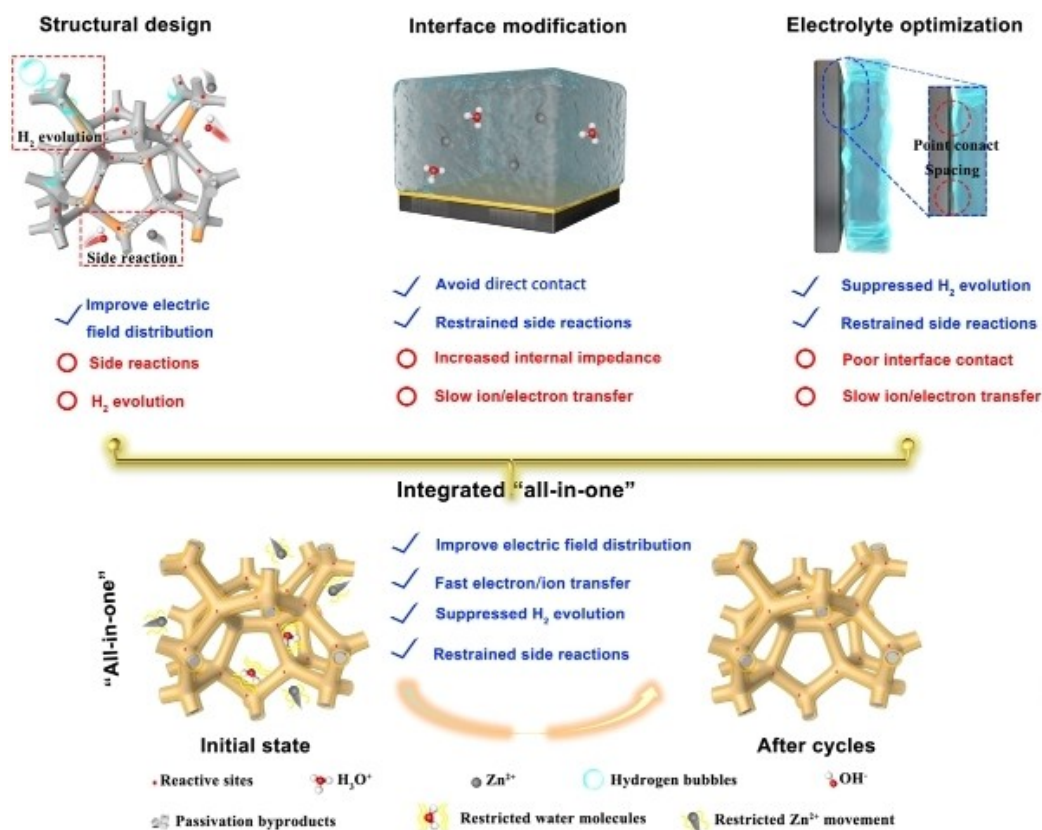
Figure 4. Structure design, electrolyte optimization and function mechanism of the "all-in-one" integrated system. Adapted with permission from Ref. [44]. Copyright (2021) Oxford University Press

3.3. Eutectic mixture

Molten salts (ionic liquid, IL) with diverse designability, thermal stability, non-flammability, wide operation voltage properties have been widely applied in electrochemical devices.[53] Eutectic mixtures are composed with two or more components, which associated with each other when the intermolecular interactions (hydrogen-bond, Lewis acid-base interaction and van der Waals forces) are stronger than the inner reactions. They have attracted much attentions in recent years because the common characterizations with IL. Furthermore, the lower ecological footprint and more cost-effectiveness than ILs give them more opportunities in EESCs.[54] The advanced functionalities of eutectic mixture exhibited in Zn battery include expanding electrochemical stability window, stabilizing electrode interface and improving cycling stability. Specifically, a judicious design of advanced eutectic mixtures should consider the solvation structure, ion transfer mechanism, electrochemical reaction pathway, advanced experimental techniques and multiscale simulation methodologies.

ZnCl₂-based eutectic mixtures (e.g., ZnCl₂/ChCl/urea, ZnCl₂/ Acetamide (Ace)) have been reported extensively in early works during the past decades.[55] Many of them demonstrate that the Zn metal could deposit and strip reversibly in these eutectic mixtures. However, the oxidation susceptibility of Cl⁻ has limited their practical applications. Recently, other Zn salts-

based eutectic mixtures, e.g., $Zn(TFSI)_2/Ace$,[56] $Zn(TFSI)_2/LiTFSI/$ urea,[57] $Zn(ClO_4)_2 \cdot 6H_2O/SN$[58] and $Zn(ClO_4)_2 \cdot 6H_2O/MSM/H_2O$,[59] have been discovered and been used as electrolyte in Zn batteries. It is confirmed that the ligand-anion-complexing solvation structure of Zn^{2+} exist in these systems. For example, the $[ZnCl(urea)]^+$, $[ZnCl(urea)_2]^+$, and $[ZnCl(urea)_3]^+$ cations in the $ZnCl_2/Urea$ system;[55a] the $[ZnTFSI(Ace)_2]^+$, $[ZnTFSI(Ace)_2]^+$, $[ZnTFSI(Ace)_3]^+$ and $[ZnTFSI(Ace)_4]^+$ in $Zn(TFSI)_2/acetamide$ system[56] (Figure 5a); the $[Zn(SN)_2]^{2+}$, $[Zn(OH_2)(SN)_2]^{2+}$, $[Zn(OH_2)_2(SN)_2]^{2+}$, $[Zn(SN)_3]^{2+}$, and $[Zn(SN)_4]^{2+}$ in $Zn(ClO_4)_2 \cdot 6H_2O/$ SN system[58](Figure 5b). Taking $Zn(TFSI)_2/Ace$ mixture as the example, the strong interactions between Zn^{2+} cation and $TFSI^-$ anion changes the de-solvation procedure and enable the uniform Zn deposition with 100% platting/stripping Coulombic efficiency even at high area capacity (2.5 mAh cm⁻²). In addition, the eutectic mixture without free water participation solves the hydrogen evolution problem and expands anodic stability limit to 2.4 V. It is totally different with that in common aqueous solution, which faces severe dendrites and side reaction issues. Furthermore, the special coordination type of the anion-complexing Zn species changes the reduction potential of $TFSI^-$. It can be reduced below 0.37 V (vs. Zn), which is much higher than that (−0.87 V) of free $TFSI^-$ in common dilute aqueous solution (Figure 5c). The *in-situ* formed ionically permeable solid electrolyte interphase (SEI) layer,
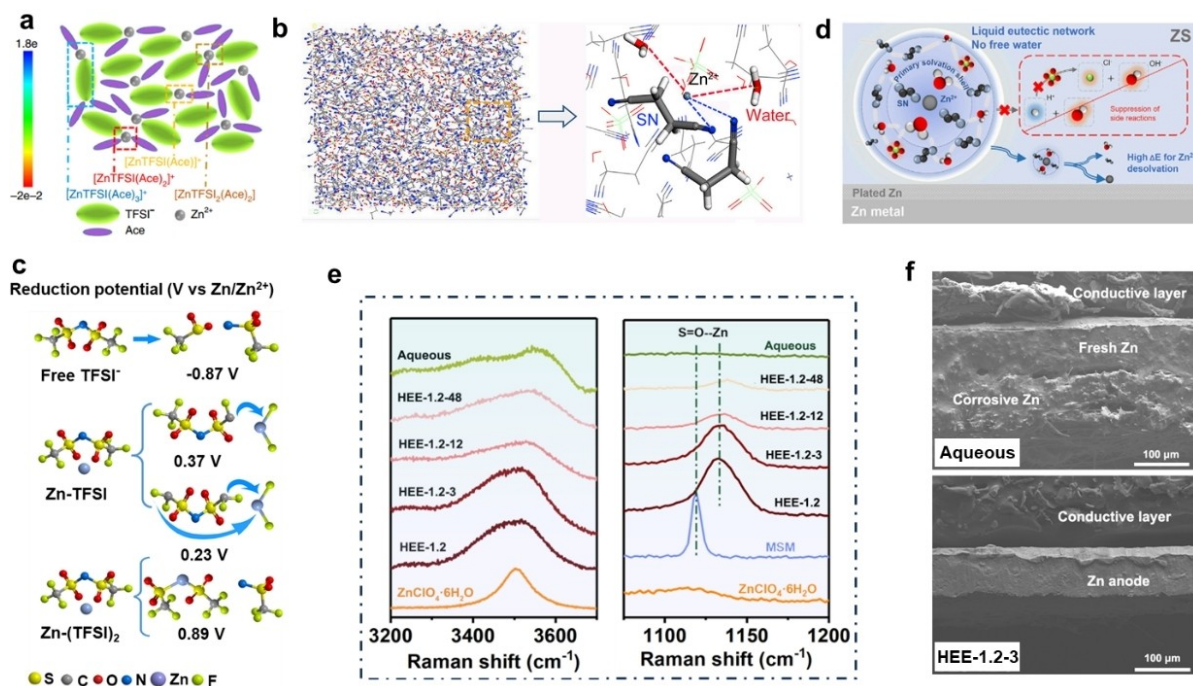
Batteries & Supercaps

Review

doi.org/10.1002/batt.202200560

Chemistry
Europe

European Chemical
Societies Publishing

Figure 5. a) Representative Zn species in Zn(TFSI)$_2$/Ace eutectic mixture. Adapted from Ref. [56]. Copyright (2019) The Author(s). Published by Springer Nature. b) Snapshot of the Zn^{2+}-solvated structure in Zn(ClO$_4$)$_2$·6H$_2$O/SN eutectic mixture. Adapted with permission from Ref. [58]. Copyright (2020) Elsevier Inc. c) Reduction potentials of TFSI$^-$ in aqueous solution and Zn(TFSI)$_2$/Ace eutectic mixture. Adapted from Ref. [56]. Copyright (2019) The Author(s). Published by Springer Nature. d) Diagrams of Zn^{2+}-solvated structure and the corresponding interfacial reactions in Zn(ClO$_4$)$_2$·6H$_2$O/SN eutectic mixture. Adapted with permission from Ref. [58]. Copyright (2020) Elsevier Inc. e) Raman characterization of Zn(ClO$_4$)$_2$·6H$_2$O/MSM/H$_2$O eutectic mixtures with different water contents; f) SEM images of Zn metal electrode after cycling in aqueous and eutectic electrolytes. Adapted with permission from Ref. [59]. Copyright (2022) Wiley-VCH.

containing ZnF$_2$ mainly, protect Zn anode from corrosion and dendrites issues.

Another example of Zn(ClO$_4$)$_2$·6H$_2$O/SN eutectic mixture share the above advanced functions in Zn batteries, such as, wide anodic stability of 2.55 V, dendrites-free and homogeneous Zn deposition, stable SEI layer and suppressed dissolution of the organic cathode. They ensure the ultralong cycling life-span of the symmetric cell (800 h) and full cell (Zn//PDB, 3500 cycles with 85.4% capacity retention) results from the advantages of this eutectic mixture electrolyte. Even though the high corrosiveness and oxidation properties of ClO$_4^-$, they are suppressed significantly because of the scarcity of free water molecules. The detailed illustration of the function mechanism of Zn(ClO$_4$)$_2$·6H$_2$O/SN mixture is shown in Figure 5(d). It is noteworthy that the usage of hydrated Zn salt and the introduction of tiny amount of water would favor the ionic conductivity. They increase from 0.31 (Zn(TFSI)$_2$/Ace eutectic mixture) to 5.52 (Zn(ClO$_4$)$_2$·6H$_2$O/SN) and 7.4 mS cm^{-1} (Zn(ClO$_4$)$_2$·6H$_2$O/MSM/H$_2$O), respectively. However, there is an upper limit of the hydration, above which the water-water and Zn^{2+}-water reactions would dominate the aqueous-eutectic hybrid mixture so that the original eutectic mixture is disturbed. Han et al.[59] have examined the inner chemical environment of Zn(ClO$_4$)$_2$·6H$_2$O/MSM/H$_2$O eutectic mixtures with different water contents. They point out that the hydrogen bonding interaction among water molecules strengthens and Zn^{2+}-S=O coordination interaction weakens significantly when

the ration among Zn salt, MSM ligand and water reaches to 1.2:3.6:12. It is a desirable point when the ratio is 1.2:3.6:3, as confirmed through Raman characterization in Figure 5(e). Compared with the aqueous electrolyte, Zn metal electrode could keep compact morphology with negligent dendrites after repeated cycles in eutectic mixture (see the SEM images in Figure 5f), which is the mechanism for extraordinary cycling stability both in half ($\geq$ 2000 hours) and full (Zn//NVO, 1600 cycles at 1 A g^{-1} almost without decay) batteries. Different with the conventional cathode used in Zn battery, Li$^+$-storage material is generally chosen to couple with Zn anode to obtain high energy outputs. Introducing Li-salt to obtain bi-salts based eutectic mixture (Zn(TFSI)$_2$/LiTFSI/urea) has been verified as compatible electrolyte with Zn. Inheriting various merits of eutectic mixture, the Zn//LiMn$_2$O$_4$ battery delivers high discharge voltage of 1.92 V, high practical energy density of 52 Wh/kg together with high-capacity retention of 90% after 300 cycles at 0.1 C.

3.4. Electrolyte additives

Zn deposition process include diffusion in diffusion layer, de-solvation and deposition steps in outer and inner Helmholtz planes because there exists diffusion and Helmholtz layers at the electrode/electrolyte interface.[60] The corresponding solvation structure, de-solvation energy barrier, charge transfer

Batteries & Supercaps

Review
doi.org/10.1002/batt.202200560

Chemistry
Europe
European Chemical
Societies Publishing

kinetic and nucleation motivation determine the fundamental technology challenges in electrolyte solution.[61] The strong interaction between water and Zn^{2+} increases the de-solvation energy barrier but favors fast diffusion. The lowest energy consumption principle in metal crystal nucleation and growth process triggers aggregated dendrites formation but keeps thermodynamic stability. The free water molecules contribute to Zn^{2+} transfer kinetic but could be reduced easily with HER before Zn deposition. One compromise of the above complicated electrochemical reaction to achieve highly efficient Zn battery is in urgent need.

Electrolyte additive strategy takes the advantages of different additives, which possesses special electron donor groups, polarity property, hydrophilic/hydrophobic property and redox reactivity, altering the Zn^{2+} solvation structure, (de)solvation energy barrier, diffusion pathways and nucleation energy.[62] In 2018, Niu and co-workers demonstrated that the Na^+ cation additive in $ZnSO_4$ electrolyte could inhibit the cathode dissolution and Zn dendrites synchronously.[63] The Zn//NVO battery delivered a high reversible capacity of 380 mAh g^{-1} with a capacity retention of 82% over 1000 cycles. One

following work further confirmed the functions of Mg^{2+} additive through both experimental and theoretical calculations.[64] It is verified that the lower adsorption energy (-1.953 eV) of Mg^{2+} than that (-0.472 eV) of Zn^{2+} at Zn surface gives it the self-healing electrostatic shield effect. It is the main reason for stopping tip electric field formation and leading to a 3D diffusion mechanism with smooth Zn deposition. In addition, there are two types of Zn^{2+}-pair species (SSIP, $Zn^{2+}(H_2O)_6SO_4^{2-}$; CIP, $Zn^{2+}(H_2O)_5OSO_3^{2-}$) in $ZnSO_4$ solution with Mg^{2+} additive due to the close binding interaction between Mg^{2+} and water. Correspondingly, the interaction between Zn^{2+} and SO_4^{2-} weakens greatly, which is conducive to restraining the SO_4^{2-} participated side reactions, the function illustration is shown in Figure 6(a). Last year, Wang and co-workers proved that the NO_3^- anion additive played a vital role in keeping the stability of Zn//MnO$_2$ cell.[65] They demonstrated that an inorganic-organic hybrid bi-layer SEI film was generated during Zn plating/stripping in the low-concentrated Zn(OTf)$_2$-Zn(NO$_3$)$_2$ electrolyte. The outer $Zn_5(OH)_8(NO_3)_2 \cdot 2H_2O$ passive layer is the result of the reaction between Zn and NO_3^-/OH^-, which is electrically and ionically resistive, preventing water
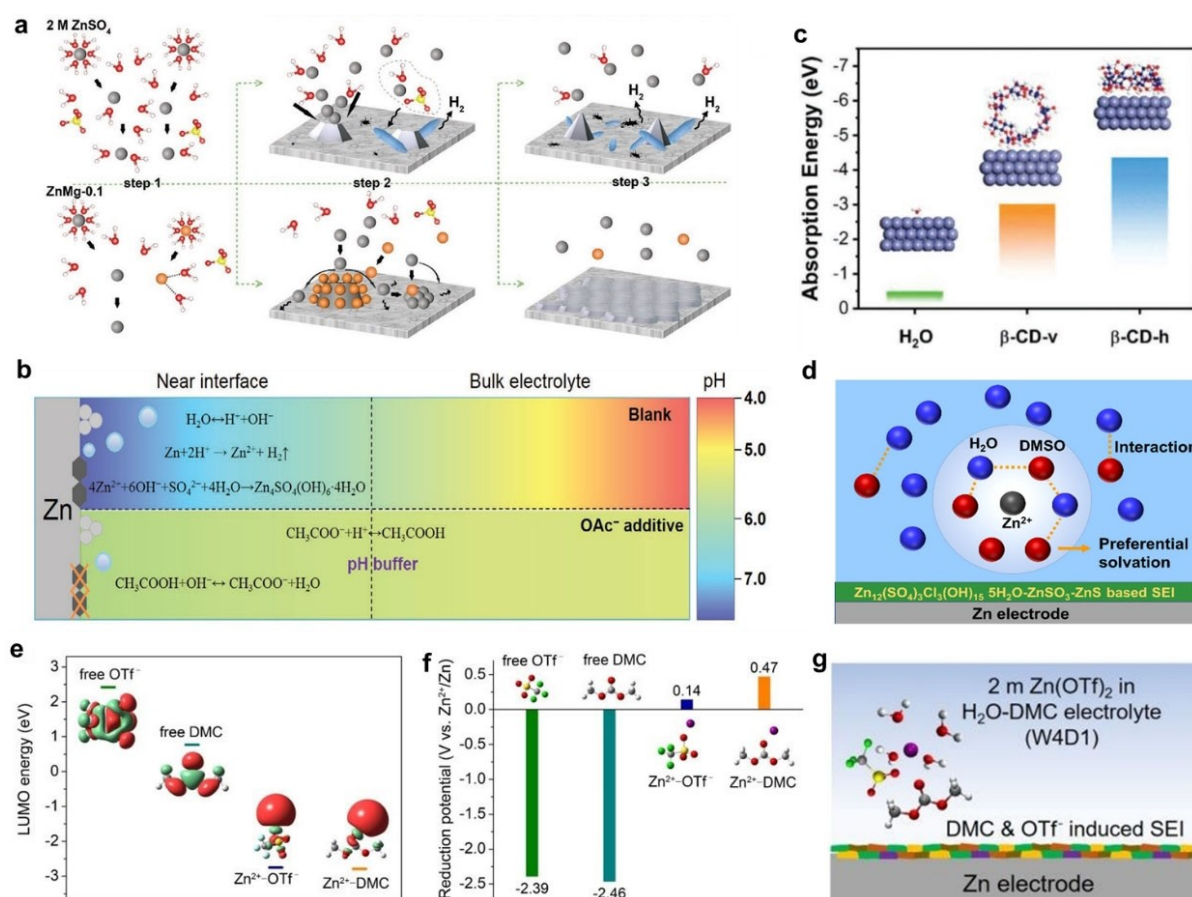

Figure 6. a) Zn deposition procedure in $ZnSO_4$ electrolyte with and without Mg^{2+} additive. Adapted with permission from Ref. [64]. Copyright (2021) Wiley-VCH. b) Different Zn/electrolyte interfacial reactions and the PH buffer mechanism of OAc$^-$ anion. Adapted with permission from Ref. [66]. Copyright (2022) Wiley-VCH. c) Adsorption energies of water and β-CD on Zn surface. Adapted with permission from Ref. [73]. Copyright (2021) Wiley-VCH. d) Illustration of the Zn^{2+}-solvated structure and the interactions between DMSO and water molecule. Adapted with permission from Ref. [72b]. Copyright (2020) American Chemical Society. e and f) LUMO energy level and the predicted reduction potential of free OTf$^-$ anion, free DMC solvent, Zn^{2+}-OTf$^-$ and Zn^{2+}-DMC composites; g) interfacial layer on Zn electrode surface in Zn(OTf)$_2$ electrolyte with DMC additive. Adapted from Ref. [74]. Copyright (2020) The Author(s). Published by Chemical Science.

Batteries & Supercaps

Review
doi.org/10.1002/batt.202200560

Chemistry Europe
European Chemical
Societies Publishing

penetrates into Zn surface. With the transformation of $Zn_5(OH)_8(NO_3)_2 \cdot 2H_2O$ to the organic protective layer of $Zn_5(OH)_6(CO_3)_2$ due to the reaction between $(CF_3SO_3)^-$ and NO_3^-, the Zn^{2+} conductive inner layer of ZnF_2 appears. The organic layer prevents SEI from crack due to dendrites growth and the hydrophobic ZnF_2 layer removes free water molecules. The finally obtained Zn//Ti asymmetric cell shows high Coulombic efficiency of 99.8% for 200 h, and the Zn//MnO₂ cell runs for 700 cycles with 96.5% capacity retention. In theory, the only electrostatic shield effect of metal cations cannot work satisfactorily because of the relevance between the PH value of electrolyte and side reactions. Considering both the dynamic electrostatic shielding layer of NH_4^+ cation and the interfacial PH buffer effect of OAc^- anion, Weng et al. reported the low-cost ammonium acetate (NH_4OAc) additive for aqueous $ZnSO_4$ electrolyte.[66] A self-regulated electrode/electrolyte interface is built in this electrolyte, where the NH_4^+ prefers to adsorb on Zn anode and suppresses agglomerative Zn deposition, and the OAc^- anion monitors H^+/OH^- concentration by the HOAc/OAc^- buffer pair. The function mechanism is shown in Figure 6(b). The more appropriate PH value (5.14) in NH_4OAc added electrolyte than that (4.10) in additive-free solution leads to suppressed side reactions (HER, Zn dendrites and insoluble by-products formation) and more stable cycling performance (3500 h at 1 mA cm⁻² with 1 mAh cm⁻²).

Organic molecules have been studied as electrolyte additives extensively because of their diversity.[67] They could adsorb on the Zn surface due to the strong interaction between Zn and polar groups in organic molecules, which improves the compatibility of Zn anode with electrolyte. Furthermore, they could engage in constructing Zn^{2+} solvation sheath and confine the free water molecules, which suppresses water-induced side reactions and widens water splitting voltage.[68] There are various kinds of organic molecule additives have been used, such as, surfactants[69] (e.g., SDS, TBA₂SO₄, SDBS), polymers[70] (e.g., PEO, PAM, PSS), chelating agent[71] (e.g., Na₄EDTA) and organic solvent (e.g., Et₂O, EG, DMC, DMSO, NMP, DMF).[29,72] Taking the sodium dodecyl sulfate (SDS) surfactant additive as an example.[69a] The wetting angle test proposes that the hydrophilic group of SDS is adsorbed on electrode surface and the hydrophobic group faces the electrolyte media. The organic layer on the cathode side could largely suppresses dissolution via blocking water from cathode material. Additionally, it requires a high energy barrier for water to pass through the dense hydrophobic layer to electrode surface, leading to higher overpotential for HER and OER with wider electrochemical stable window (2.5 V). Polymers and chelating agents possessing various functional groups (–NH₂, –C–O, –S–O) and covalent bonded units could induce distinctive interactions with Zn anode, Zn^{2+} ion and water molecules.[73] Taking the β-cyclodextrin (β-CD) as an example (Figure 6c), β-CD molecule shows much higher adsorption energy at Zn surface than water, indicating the stronger interactions between them. They contribute to solvation sheath re-construction, changing diffusion pathways of solvated Zn^{2+} ion, regulating electrolyte PH value and nucleation overpotential. It is to be noted that the organic solvent is the most studied

organic molecule additive because of the high solubility and low-cost properties. As shown in Figure 6(d), DMSO molecule could enter into the primary sheath of Zn^{2+} and form intermolecular bonds with water. Apart from the high Gutmann donor number property, which is important to re-constructure Zn^{2+} solvation sheath, and the strong hydrogen bonding interaction with water, which is indispensable to restrict water activity. DMSO molecule is able to form a dense and self-repairable SEI layer on Zn surface to stop side reactions. Wang and co-workers[72b] demonstrated that both the well-identified characteristic peaks in the XRD spectra and XPS with Ar^+ sputtering depth profiling characterization suggest that the $Zn_{12}(SO_4)_3Cl_3(OH)_{15}$-$ZnSO_3$-ZnS SEI layer forms on Zn anode in $ZnCl_2$-DMSO electrolyte. It enables the successful operation of electrochemical reactions but blocks water-induced side reactions. Zhang and co-workers[74] further prove that both the LUMO energy and reduction potential of OTf^- and DMC are lowered when they coordinate with Zn^{2+} in the $Zn(OTf)_2$-DMC solution (Figure 6e and f). Correspondingly, a robust ZnF_2 and $ZnCO_3$-rich interphase forms and modifies the Zn surface, as illustrated in Figure 6(g). It makes sure the high Coulombic efficiency of Zn plating/stripping and dendrite-free cycling over 1000 cycles. Up to now, various works about the organic molecule additives have proved its function in aqueous Zn battery (Table S1). More kinds of low-cost and effective additives maybe found in near future for more advanced Zn battery.

4. Conclusion and Outlook

Although aqueous Zn battery is regarded as a promising kind of environment-friendly and cost-effective energy storage technology, the severe parasitic side reactions associated with water molecules limit the large-scale application. The issues faced by Zn battery include narrow electrochemical window, low energy density, Zn dendrite growth, Zn metal corrosion, and inferior cycling stability. Taking serious consideration of the challenges, various electrolyte modulation strategies aimed to reduce water solvent content and suppress water activity have been employed. The typical methods discussed in this review are hybrid/concentrated solution, gel polymer electrolyte (hydrogel electrolyte), eutectic mixture, and electrolyte additive strategies. Through enhancing interfacial compatibility, covering electrode surface with SEI layer, altering solvation structure of Zn^{2+}, and regulating diffusion pathways of solvated Zn^{2+}, enormous progresses in aqueous Zn battery have been achieved. They are listed as follows: 1) Widening the ESW up to ~3 V; 2) Improving the energy density; 3) Highly safe operation; 4) Ultra-long cycling stability. A comparison of electrochemical performance of Zn batteries based on different electrolyte modulation strategies is shown in SI information. Apart from the anode and electrolyte aspects, the positive effect of electrolyte modulation strategy also appears at cathode side. On one hand, some cathode materials (e.g., Mn_xO_y, VO_x) are very sensitive to aqueous solution and the pH environment of the electrolyte. The above strategies could prohibit H_2O-

participated side reactions effectively through limiting water activity and changing inner chemical environment of the electrolyte. On the other hand, the modified solvation structure of the charge carrier changes the diffusion pathways, solvation/de-solvation procedures and charge-transfer reactions, stabilizing the cathode materials. Additionally, a dissolution balance of the cathode materials could also be achieved through these modulation methods, which is vital but cannot be ignored in any electrochemical reactions.

Compared with traditional aqueous solution, the concentrated solution is more effective to decrease the free-water molecule content to reach the high-energy density target. However, most of them with extra costly fluorinated metal salts compromise the economic and environment requirements of Zn battery. Additionally, the high viscosity and low ionic conductivity result in poor rate performance and low energy efficiency. It is increasingly popular to solve the above issues of aqueous Zn battery by employing polymeric hydrogels, especially for flexible device development. The polymeric hydrogel strategy enables to improves the comprehensive performance of Zn battery and is indispensable for flexible devices. Thus, research on designing advanced hydrogels with specific functionalities (e.g., stretchability, foldability, self-healing ability, wearability and biocompatibility) for wide applications in the future are required. The concept of eutectic mixture seems straightforward because of the advantageous features of feasible design, tunable composition, thermal/electrochemical stability, and high safety. Nonetheless, research on eutectic mixture is still in its infancy stage. The best matched salt-ligand combinations and the deep understanding on their solution structure, electrical structure, charge transfer mechanism and interface chemistry require systematic investigations. Electrolyte additives could equalize surface energy and guide ion flux along Zn anode; occupy the primary solvation shell of Zn^{2+} and poll out solvated water molecule; coordinate with Zn^{2+} to be reduced with SEI formation; and construct hydrogen bonds with free water to restrict their activity. Until now, it is the most reported strategy being used. Moreover, some universal principles to guide electrolyte additive strategy for better Zn batteries have been put forward: 1) cost-effective and non-toxic, which is required by the concept of the future low-cost EESCs; 2) more prone to corporate with Zn^{2+} than water, which is critical to guide ion flux and alter solvation structure of Zn^{2+}; 3) be able to break original hydrogen bonds in water clusters, which contributes to suppress water activity and HER reaction; 4) be electrostatic shielding effective, which is usually the property of cation ion additives to modulate the Zn nucleation procedure; 5) be better if it could be electrochemically reduced easily, which leads to SEI layer formation for better electrode protection. However, there still exist some open questions to be addressed: 1) cycling stability of symmetric cell at high current density with high area capacity should be tested; 2) uniform evaluation criteria (e.g., the volume of electrolyte, the thickness of Zn metal, testing methods, current density) should be set; 3) deep electrochemical reaction mechanism (e.g., ion diffusion and charge transfer mechanism, (de)solvation process, solvation structure) should be studied.

Acknowledgements

Conflict of Interest

The authors declare no conflict of interest.

[1] a) M. Li, J. Lu, Z. Chen, K. Amine, *Adv. Mater.* **2018**, e1800561; b) M. Armand, J.-M. Tarascon, *Nature* **2008**, *451*, 652–657; c) Y. Dai, X. Liao, R. Yu, J. Li, J. Li, S. Tan, P. He, Q. An, Q. Wei, L. Chen, X. Hong, K. Zhao, Y. Ren, J. Wu, Y. Zhao, L. Mai, *Adv. Mater.* **2021**, *33*, e2100359.

[2] a) Wu Li, J. R. Dahn, D. S. Wainwright, *Science*, *264*, 1115–1118; b) M. Lao, Y. Zhang, W. Luo, Q. Yan, W. Sun, S. X. Dou, *Adv. Mater.* **2017**, *29*, 1700622; c) W. Zong, N. Chui, Z. Tian, Y. Li, C. Yang, D. Rao, W. Wang, J. Huang, J. Wang, F. Lai, T. Liu, *Adv. Sci.* **2021**, *8*, 2004142.

[3] a) S.-W. Kim, D.-H. Seo, X. Ma, G. Ceder, K. Kang, *Adv. Energy Mater.* **2012**, *2*, 710–721; b) L. Jiang, Y. Lu, C. Zhao, L. Liu, J. Zhang, Q. Zhang, X. Shen, J. Zhao, X. Yu, H. Li, X. Huang, L. Chen, Y.-S. Hu, *Nat. Energy* **2019**, *4*, 495–503; c) W. Zong, H. Guo, Y. Ouyang, L. Mo, C. Zhou, G. Chao, J. Hofkens, Y. Xu, W. Wang, Y. E. Miao, G. He, I. P. Parkin, F. Lai, T. Liu, *Adv. Funct. Mater.* **2022**, *32*, 2110016.

[4] a) M. Mao, T. Gao, S. Hou, C. Wang, *Chem. Soc. Rev.* **2018**, *47*, 8804–8841; b) Z. A. Zafar, S. Imtiaz, R. Razaq, S. Ji, T. Huang, Z. Zhang, Y. Huang, J. A. Anderson, *J. Mater. Chem. A* **2017**, *5*, 5646–5660.

[5] a) C. Xu, B. Li, H. Du, F. Kang, *Angew. Chem. Int. Ed.* **2012**, *51*, 933–935; *Angew. Chem.* **2012**, *124*, 957–959; b) R. C. Massé, C. Liu, Y. Li, L. Mai, G. Cao, *Natl. Sci. Rev.* **2017**, *4*, 26–53.

[6] Y. Wang, Z. Wang, F. Yang, S. Liu, S. Zhang, J. Mao, Z. Guo, *Small* **2022**, *18*, e2107033.

[7] a) L. Geng, X. Wang, K. Han, P. Hu, L. Zhou, Y. Zhao, W. Luo, L. Mai, *ACS Energy Lett.* **2021**, *7*, 247–260; b) H. Li, R. Meng, Y. Guo, B. Chen, Y. Jiao, C. Ye, Y. Long, A. Tadich, Q. H. Yang, M. Jaroniec, S. Z. Qiao, *Nat. Commun.* **2021**, *12*, 5714.

[8] C. Dong, H. Kobayashi, I. Honma, *Mater. Today Energy* **2022**, *30*, 101143.

[9] a) X. Jia, C. Liu, Z. G. Neale, J. Yang, G. Cao, *Chem. Rev.* **2020**, *120*, 7795–7866; b) Q. Zhao, W. Huang, Z. Luo, L. Liu, Y. Lu, Y. Li, L. Li, J. Hu, H. Ma, J. Chen, *Sci. Adv.* **2018**, *4*, eaao1761.

[10] a) Q. Li, Y. Qiao, S. Guo, K. Jiang, Q. Li, J. Wu, H. Zhou, *Joule* **2018**, *2*, 1134–1145; b) L. Kang, M. Cui, Z. Zhang, F. Jiang, *Batteries & Supercaps* **2020**, *3*, 966–1005.

[11] a) M. Han, L. Qin, Z. Liu, L. Zhang, X. Li, B. Lu, J. Huang, S. Liang, J. Zhou, *Mater. Today Energy* **2021**, *20*, 100626; b) M. Han, J. Huang, S. Liang, L. Shan, X. Xie, Z. Yi, Y. Wang, S. Guo, J. Zhou, *iScience* **2020**, *23*, 100797.

[12] a) L. Ma, M. A. Schroeder, T. P. Pollard, O. Borodin, M. S. Ding, R. Sun, L. Cao, J. Ho, D. R. Baker, C. Wang, K. Xu, *Energy Environ. Mater.* **2020**, *3*, 516–521; b) C. Zhang, W. Shin, L. Zhu, C. Chen, J. C. Neuefeind, Y. Xu, S. I. Allec, C. Liu, Z. Wei, A. Daniyar, J. X. Jiang, C. Fang, P. A. Greaney, X. Ji, *Carbon Energy* **2020**, *3*, 339–348; c) T. Zhang, Y. Tang, S. Guo, X. Cao, A. Pan, G. Fang, J. Zhou, S. Liang, *Energy Environ. Sci.* **2020**, *13*, 4625–4665.

[13] D. Chao, S.-Z. Qiao, *Joule* **2020**, *4*, 1846–1851.

[14] L. Suo, O. Borodin, T. Gao, M. Olguin, J. Ho, X. Fan, C. Luo, C. Wang, K. Xu, *Sincece* **2015**, *350*, 938–943.

[15] a) D. Chao, W. Zhou, F. Xie, C. Ye, H. Li, M. Jaroniec, S.-Z. Qi, *Sci. Adv.* **2020**, *6*; b) A. Eftekhari, *Adv. Energy Mater.* **2018**, *8*, 1801156.

[16] S. Liu, R. Zhang, J. Mao, Y. Zhao, Q. Cai, Z. Guo, *Sci. Adv.* **2022**, *8*, eabn5097.

[17] a) L. Ma, M. A. Schroeder, O. Borodin, T. P. Pollard, M. S. Ding, C. Wang, K. Xu, *Nat. Energy* **2020**, *5*, 743–749; b) J. Zheng, Q. Zhao, T. Tang, J. Yin, C. D. Quilty, G. D. Renderos, X. Liu, Y. Deng, L. Wang, D. C. Bock, C. Jaye, D. Zhang, E. S. Takeuchi, K. J. Takeuchi, A. C. Marschilok, L. A. Archer, *Science* **2019**, *366*, 645–648; c) V. Verma, S. Kumar, W. Manalastas, M. Srinivasan, *ACS Energy Lett.* **2021**, *6*, 1773–1785.

[18] a) Y. Zhang, J. D. Howe, Y. Ben-Yoseph, Y. Wu, N. Liu, *ACS Energy Lett.* **2021**, *6*, 404–412; b) C. Liu, X. Xie, B. Lu, J. Zhou, S. Liang, *ACS Energy Lett.* **2021**, *6*, 1015–1033; c) Q. Zhang, Y. Ma, Y. Lu, L. Li, F. Wan, K. Zhang, J. Chen, *Nat. Commun.* **2020**, *11*, 4463; d) X. Zeng, J. Mao, J. Hao, J. Liu, S. Liu, Z. Wang, Y. Wang, S. Zhang, T. Zheng, J. Liu, P. Rao, Z. Guo, *Adv. Mater.* **2021**, *33*, e2007416.

[19] a) J. Yan, E. H. Ang, Y. Yang, Y. Zhang, M. Ye, W. Du, C. C. Li, *Adv. Funct. Mater.* **2021**, *31*, 2010213; b) C. Wu, H. Tan, W. Huang, W. Li, K. N. Dinh, C. Yan, W. Wei, L. Chen, Q. Yan, *Adv. Funct. Mater.* **2020**, 2003187.

[20] a) C. Deng, X. Xie, J. Han, Y. Tang, J. Gao, C. Liu, X. Shi, J. Zhou, S. Liang, *Adv. Funct. Mater.* **2020**, *30*, 2000599; b) L. Yan, X. Zeng, Z. Li, X. Meng, D. Wei, T. Liu, M. Ling, Z. Lin, C. Liang, *Mater. Today Energy* **2019**, *13*, 323–330.

[21] Y. Zhu, J. Yin, X. Zheng, A.-H. Emwas, Y. Lei, O. F. Mohammed, Y. Cui, H. N. Alshareef, *Energy Environ. Sci.* **2021**, *14*, 4463–4473.

[22] a) T. Liang, R. Hou, Q. Dou, H. Zhang, X. Yan, *Adv. Funct. Mater.* **2020**; b) F. Ming, Y. Zhu, G. Huang, A. H. Emwas, H. Liang, Y. Cui, H. N. Alshareef, *J. Am. Chem. Soc.* **2022**, *144*, 7160–7170.

[23] P. Senguttuvan, S.-D. Han, S. Kim, A. L. Lipson, S. Tepavcevic, T. T. Fister, I. D. Bloom, A. K. Burrell, C. S. Johnson, *Adv. Energy Mater.* **2016**, *6*, 1600826.

[24] A. S. Etman, M. Carboni, J. Sun, R. Younesi, *Energy Technol.* **2020**, *8*, 2000358.

[25] a) A. Naveed, H. Yang, Y. Shao, J. Yang, N. Yanna, J. Liu, S. Shi, L. Zhang, A. Ye, B. He, J. Wang, *Adv. Mater.* **2019**, *31*, e1900668; b) Z. Chen, Y. Tang, X. Du, B. Chen, G. Lu, X. Han, Y. Zhang, W. Yang, P. Han, J. Zhao, G. Cui, *Angew. Chem. Int. Ed.* **2020**, *59*, 21769–21777; *Angew. Chem.* **2020**, *132*, 21953–21961.

[26] L. Ma, J. Vatamanu, N. T. Hahn, T. P. Pollard, O. Borodin, V. Petkov, M. A. Schroeder, Y. Ren, M. S. Ding, C. Luo, J. L. Allen, C. Wang, K. Xu, *Proc. Nat. Acad. Sci.* **2022**, *119*, e2121138119.

[27] S. Liu, J. P. Vongsvivut, Y. Wang, R. Zhang, F. Yang, S. Zhang, K. Davey, J. Mao, Z. Guo, *Angew. Chem. Int. Ed.* **2023**, *62*, e202215600.

[28] A. Naveed, H. Yang, J. Yang, Y. Nuli, J. Wang, *Angew. Chem. Int. Ed.* **2019**, *58*, 2760–2764; *Angew. Chem.* **2019**, *131*, 2786–2790.

[29] R. Qin, Y. Wang, M. Zhang, Y. Wang, S. Ding, A. Song, H. Yi, L. Yang, Y. Song, Y. Cui, J. Liu, Z. Wang, S. Li, Q. Zhao, F. Pan, *Nano Energy* **2021**, *80*, 105478.

[30] F. Wang, O. Borodin, T. Gao, X. Fan, W. Sun, F. Han, A. Faraone, J. A. Dura, K. Xu, C. Wang, *Nat. Mater.* **2018**, *17*, 543–549.

[31] a) Q. Ni, H. Jiang, S. Sandstrom, Y. Bai, H. Ren, X. Wu, D. Y. Q. Guo, C. Wu, X. Ji, *Adv. Funct. Mater.* **2020**, 2003511; b) C. Zhang, J. Holoubek, X. Wu, A. Daniyar, L. Zhu, C. Chen, D. P. Leonard, I. A. Rodríguez-Pérez, J. X. Jiang, C. Fang, X. Ji, *Chem. Commun.* **2018**, *54*, 14097.

[32] S. Tang, W. Guo, Y. Fu, *Adv. Energy Mater.* **2020**, *11*, 2000802.

[33] a) P. Yu, Y. Zeng, H. Zhang, M. Yu, Y. Tong, X. Lu, *Small* **2019**, *15*, e1804760; b) Z. Liu, F. Mo, H. Li, M. Zhu, Z. Wang, G. Liang, C. Zhi, *Small Methods* **2018**, *2*, 1800124.

[34] a) L. Ma, S. Chen, N. Li, Z. Liu, Z. Tang, J. A. Zapien, S. Chen, J. Fan, C. Zhi, *Adv. Mater.* **2020**, *32*, e1908121; b) Z. Wang, H. Li, Z. Tang, Z. Liu, Z. Ruan, L. Ma, Q. Yang, D. Wang, C. Zhi, *Adv. Funct. Mater.* **2018**, *28*, 1804560; c) M. Wu, Y. Zhang, L. Xu, C. Yang, M. Hong, M. Cui, B. C. Clifford, S. He, S. Jing, Y. Yao, L. Hu, *Matter* **2022**, *5*, 3402–3416.

[35] a) L. Sun, Y. Yao, L. Dai, M. Jiao, B. Ding, Q. Yu, J. Tang, B. Liu, *Energy Storage Mater.* **2022**, *47*, 187–194; b) K. Wu, J. Huang, J. Yi, X. Liu, Y. Liu, Y. Wang, J. Zhang, Y. Xia, *Adv. Energy Mater.* **2020**, *10*, 1903977.

[36] X. Zeng, K. Xie, S. Liu, S. Zhang, J. Hao, J. Liu, W. K. Pang, J. Liu, P. Rao, Q. Wang, J. Mao, Z. Guo, *Energy Environ. Sci.* **2021**, *14*, 5947–5957.

[37] Z. Liu, D. Wang, Z. Tang, G. Liang, Q. Yang, H. Li, L. Ma, F. Mo, C. Zhi, *Energy Storage Mater.* **2019**, *23*, 636–645.

[38] J. Zhu, M. Yao, S. Huang, J. Tian, Z. Niu, *Angew. Chem. Int. Ed.* **2020**, *59*, 16480–16484; *Angew. Chem.* **2020**, *132*, 16622–16626.

[39] Y. Meng, L. Zhang, M. Peng, D. Shen, C. Zhu, S. Qian, J. Liu, Y. Cao, C. Yan, J. Zhou, T. Qian, *Adv. Funct. Mater.* **2022**, *32*, 2206653.

[40] S. Huang, L. Hou, T. Li, Y. Jiao, P. Wu, *Adv. Mater.* **2022**, *34*, e2110140.

[41] Y. Zeng, X. Zhang, Y. Meng, M. Yu, J. Yi, Y. Wu, X. Lu, Y. Tong, *Adv. Mater.* **2017**, *29*, 1700274.

[42] H. Li, C. Han, Y. Huang, Y. Huang, M. Zhu, Z. Pei, Q. Xue, Z. Wang, Z. Liu, Z. Tang, Y. Wang, F. Kang, B. Li, C. Zhi, *Energy Environ. Sci.* **2018**, *11*, 941–951.

[43] J. Y. Sun, X. Zhao, W. R. Illeperuma, O. Chaudhuri, K. H. Oh, D. J. Mooney, J. J. Vlassak, Z. Suo, *Nature* **2012**, *489*, 133–136.

[44] C. Li, X. Xie, H. Liu, P. Wang, C. Deng, B. Lu, J. Zhou, S. Liang, *Natl. Sci. Rev.* **2021**, *9*, nwab177.

[45] F. Mo, Z. Chen, G. Liang, D. Wang, Y. Zhao, H. Li, B. Dong, C. Zhi, *Adv. Energy Mater.* **2020**, *10*, 2000035.

[46] M. Johnsi, S. A. Suthanthiraraj, *High Perform. Polym.* **2015**, *27*, 877–885.

[47] J. P. T. Guisao, A. J. F. Romero, *Electrochim. Acta* **2015**, *176*, 1447–1453.

[48] H. Dong, J. Li, S. Zhao, F. Zhao, S. Xiong, D. J. L. Brett, G. He, I. P. Parkin, *J. Mater. Chem. A* **2020**, *8*, 22637–22644.

[49] V. Vijayakumar, M. Ghosh, M. Kurian, A. Torris, S. Dilwale, M. V. Badiger, M. Winter, J. R. Nair, S. Kurungot, *Small* **2020**, *16*, e2002528.

[50] S. Karan, M. Sahu, T. B. Sahu, Y. K. Mahipal, D. K. Sahu, R. C. Agrawal, *Mater. Today Commun.* **2017**, *13*, 269–274.

[51] D. Lin, W. Liu, Y. Liu, H. R. Lee, P. C. Hsu, K. Liu, Y. Cui, *Nano Lett.* **2016**, *16*, 459–465.

[52] J. Gao, X. Xie, S. Liang, B. Lu, J. Zhou, *Nano-Micro Lett.* **2021**, *13*, 69.

[53] M. Watanabe, M. L. Thomas, S. Zhang, K. Ueno, T. Yasuda, K. Dokko, *Chem. Rev.* **2017**, *117*, 7190–7239.

[54] a) E. L. Smith, A. P. Abbott, K. S. Ryder, *Chem. Rev.* **2014**, *114*, 11060–11082; b) Q. Zhang, K. De Oliveira Vigier, S. Royer, F. Jerome, *Chem. Soc. Rev.* **2012**, *41*, 7108–7146; c) C. Zhang, L. Zhang, G. Yu, *Acc. Chem. Res.* **2020**, *53*, 1648–1659; d) J. Xu, X. Ji, J. Zhang, C. Yang, P. Wang, S. Liu, K. Ludwig, F. Chen, P. Kofinas, C. Wang, *Nat. Energy* **2022**, *7*, 186–193.

[55] a) W. Kao-ian, R. Pornprasertsuk, P. Thamyongkit, T. Maiyalagan, S. Kheawhom, *J. Electrochem. Soc.* **2019**, *166*, A1063–A1069; b) N. S. Venkata Narayanan, B. V. Ashokraj, S. Sampath, *J. Colloid Interface Sci.* **2010**, *342*, 505–512.

[56] H. Qiu, X. Du, J. Zhao, Y. Wang, J. Ju, Z. Chen, Z. Hu, D. Yan, X. Zhou, G. Cui, *Nat. Commun.* **2019**, *10*, 5374.

[57] J. Zhao, J. Zhang, W. Yang, B. Chen, Z. Zhao, H. Qiu, S. Dong, X. Zhou, G. Cui, L. Chen, *Nano Energy* **2019**, *57*, 625–634.

[58] W. Yang, X. Du, J. Zhao, Z. Chen, J. Li, J. Xie, Y. Zhang, Z. Cui, Q. Kong, Z. Zhao, C. Wang, Q. Zhang, G. Cui, *Joule* **2020**, *4*, 1557–1574.

[59] M. Han, J. Huang, X. Xie, T. C. Li, J. Huang, S. Liang, J. Zhou, H. J. Fan, *Adv. Funct. Mater.* **2022**, *32*, 2110957.

[60] a) D. Yuan, J. Zhao, H. Ren, Y. Chen, R. Chua, E. T. J. Jie, Y. Cai, E. Edison, W. Manalastas, Jr., M. W. Wong, M. Srinivasan, *Angew. Chem. Int. Ed.* **2021**, *60*, 7213–7219; *Angew. Chem.* **2021**, *133*, 7289–7295; b) J.-C. Liu, Z.-H. Huang, T.-Y. Ma, *Small Struct.* **2020**, *1*, 2000020; c) X. Liu, P. Wang, X. Liang, Q. Zhang, Z. Wang, Y. Liu, Z. Zheng, Y. Dai, B. Huang, *Mater. Today Energy* **2020**, *18*, 100524.

[61] a) S. Liu, J. Mao, W. K. Pang, J. Vongsvivut, X. Zeng, L. Thomsen, Y. Wang, J. Liu, D. Li, Z. Guo, *Adv. Funct. Mater.* **2021**, *31*, 2104281; b) J. Cao, D. Zhang, X. Zhang, Z. Zeng, J. Qin, Y. Huang, *Energy Environ. Sci.* **2022**, *15*, 499–528; c) Q. Zhang, Y. Ma, Y. Lu, Y. Ni, L. Lin, Z. Hao, Z. Yan, Q. Zhao, J. Chen, *J. Am. Chem. Soc.* **2022**, *144*, 18435–18443.

[62] a) Z. Ye, Z. Cao, M. O. Lam Chee, P. Dong, P. M. Ajayan, J. Shen, M. Ye, *Energy Storage Mater.* **2020**, *32*, 290–305; b) T. C. Li, D. Fang, J. Zhang, M. E. Pam, Z. Y. Leong, J. Yu, X. L. Li, D. Yan, H. Y. Yang, *J. Mater. Chem. A* **2021**, *9*, 6013–6028; c) S. Huang, J. Zhu, J. Tian, Z. Niu, *Chemistry* **2019**, *25*, 14480–14494.

[63] F. Wan, L. Zhang, X. Dai, X. Wang, Z. Niu, J. Chen, *Nat. Commun.* **2018**, *9*, 1656–1666.

[64] P. Wang, X. Xie, Z. Xing, X. Chen, G. Fang, B. Lu, J. Zhou, S. Liang, H. J. Fan, *Adv. Energy Mater.* **2021**, *11*, 2101158.

[65] D. Li, L. Cao, T. Deng, S. Liu, C. Wang, *Angew. Chem. Int. Ed.* **2021**, *60*, 13035–13041; *Angew. Chem.* **2021**, *133*, 13145–13151.

[66] D. Han, Z. Wang, H. Lu, H. Li, C. Cui, Z. Zhang, R. Sun, C. Geng, Q. Liang, X. Guo, Y. Mo, X. Zhi, F. Kang, Z. Weng, Q. H. Yang, *Adv. Energy Mater.* **2022**, *12*, 2102982.

[67] a) J. Xie, Z. Liang, Y. C. Lu, *Nat. Mater.* **2020**, *19*, 1006–1011; b) D. Wang, Q. Li, Y. Zhao, H. Hong, H. Li, Z. Huang, G. Liang, Q. Yang, C. Zhi, *Adv. Energy Mater.* **2022**, *12*, 2102707; c) S. Guo, L. Qin, T. Zhang, M. Zhou, J. Zhou, G. Fang, S. Liang, *Energy Storage Mater.* **2021**, *34*, 545–562.

[68] H. Huang, D. Xie, J. Zhao, P. Rao, W. M. Choi, K. Davey, J. Mao, *Adv. Energy Mater.* **2022**, *12*, 2202419.

[69] a) Z. Hou, X. Zhang, X. Li, Y. Zhu, J. Liang, Y. Qian, *J. Mater. Chem. A* **2017**, *5*, 730–738; b) J. Hao, J. Long, B. Li, X. Li, S. Zhang, F. Yang, X. Zeng, Z. Yang, W. K. Pang, Z. Guo, *Adv. Funct. Mater.* **2019**, *29*, 1903605; c) A. Bayaguud, X. Luo, Y. Fu, C. Zhu, *ACS Energy Lett.* **2020**, *5*, 3012–3020.

[70] a) Y. Jin, K. S. Han, Y. Shao, M. L. Sushko, J. Xiao, H. Pan, J. Liu, *Adv. Funct. Mater.* **2020**, *30*, 2003932; b) M. Yan, N. Dong, X. Zhao, Y. Sun, H. Pan, *ACS Energy Lett.* **2021**, *6*, 3236–3243; c) Q. Zhang, J. Luan, L. Fu, S. Wu, Y. Tang, X. Ji, H. Wang, *Angew. Chem. Int. Ed.* **2019**, *58*, 15841–15847; *Angew. Chem.* **2019**, *131*, 15988–15994.

[71] S. J. Zhang, J. Hao, D. Luo, P. F. Zhang, B. Zhang, K. Davey, Z. Lin, S. Z. Qiao, *Adv. Energy Mater.* **2021**, *11*, 2102010.

[72] a) B. Wang, R. Zheng, W. Yang, X. Han, C. Hou, Q. Zhang, Y. Li, K. Li, H. Wang, *Adv. Funct. Mater.* **2022**, 2112693; b) L. Cao, D. Li, E. Hu, J. Xu, T. Deng, L. Ma, Y. Wang, X. Q. Yang, C. Wang, *J. Am. Chem. Soc.* **2020**, *142*, 21404–21409; c) P. Sun, L. Ma, W. Zhou, M. Qiu, Z. Wang, D. Chao, W. Mai, *Angew. Chem. Int. Ed.* **2021**, *60*, 18247–18255; *Angew. Chem.* **2021**, *133*, 18395–18403; d) W. Xu, K. Zhao, W. Huo, Y. Wang, G. Yao, X. Gu, H. Cheng, L. Mai, C. Hu, X. Wang, *Nano Energy* **2019**, *62*, 275–281; e) C. Li,

A. Shyamsunder, A. G. Hoane, D. M. Long, C. Y. Kwok, P. G. Kotula, K. R. Zavadil, A. A. Gewirth, L. F. Nazar, *Joule* **2022**, *6*, 1103–1120.

[73] C. Meng, W. He, L. Jiang, Y. Huang, J. Zhang, H. Liu, J. J. Wang, *Adv. Funct. Mater.* **2022**, *32*, 2207732.

[74] Y. Dong, L. Miao, G. Ma, S. Di, Y. Wang, L. Wang, J. Xu, N. Zhang, *Chem. Sci.* **2021**, *12*, 5843–5852.